## PAPER

Check for updates

# Carbon-paste nanocomposites as unconventional gate electrodes for electrolyte-gated organic field-effect transistors: electrical modulation and bio-sensing†

Jose Muñoz, [ID] [a] Francesca Leonardi, [ID] [a] Tayfun Özmen, [a] Marta Riba-Moliner, [ID] [a] Arantzazu González-Campo, [ID] [a] Mireia Baeza [ID] [b] and Marta Mas-Torrent [ID] ★[ac]

Nanocomposite carbon-paste electrodes (NC-CPEs) have been investigated for the first time in electrolyte-gated organic field-effect transistors (EGOFETs) as a replacement of conventional metal gate electrodes, using carbon nanotubes (CNTs) as a model carbon filler. Interestingly, the electrical properties of the resulting devices have been modulated by changing the loading percentage of CNTs within the insulating polymeric matrix. The potential of using such non-conventional gate electrodes for sensing purposes has also been evaluated by investigating, as a proof of concept, the formation of a supramolecular complex between a functionalized CNT-based NC-CPE containing β-cyclodextrin (β-CD) as a bio-recognition element and tryptophan (TRP). This approach, in synergism with the amplification function of an EGOFET, affords a shift in the threshold voltage ($V_{TH}$) of the transistor, giving promising analytical results with detection limits at picomolar levels ($1.0 \pm 0.1$ pM) as well as a linear response from $10^{-12}$ to $10^{-9}$ M. Accordingly, NC-CPEs have been demonstrated to be a potential alternative to metal gate electrodes for the development of a new generation of highly sensitive carbon-based EGOFET bio-sensors.

Electrolyte-gated organic field-effect transistors (EGOFETs) are one of the most promising technologies in the field of bio-electronics.[1–3] EGOFETs are three-terminal electronic devices consisting of two electrodes (source, S, and drain, D) connected throughout a thin organic semiconducting (OSC) layer. The OSC is covered by an electrolyte solution that acts as a dielectric, where a third electrode (gate, G) is immersed. The operation principle is based on tuning the electrical current flowing along the OSC by the application of a gate voltage that leads to the formation of two electrical double layers at the OSC/electrolyte and electrolyte/gate interfaces.[4] The main advantage of this technology is the possibility to work in water or buffered media at low voltages (<1 V), permitting its direct application in the field of bio-sensing since the biological agents remain active.[5,6]

Interfaces are pivotal for ruling the EGOFET operation and are exploited for the development of sensors. From an electro-analytical point of view, the key point to achieve a highly sensitive EGOFET bio-recognition platform relies on the possibility of properly functionalizing either the gate electrode or the OSC, the two electronic active interfaces of the transistor.[7] Engineering of the gate electrode/electrolyte interface by means of binding a proper bio-receptor has been demonstrated to be a viable route in bio-sensing.[8–10] The formation of a host–guest supramolecular interaction between the target analyte and the anchored bio-receptor changes the potential of the gate electrode ($V_{GS}$), affecting directly the current flowing between the S–D electrodes ($I_{DS}$) due to a threshold voltage ($V_{TH}$) shift.

Gate electrodes with high specific surface area are desirable for a high current modulation in EGOFETs. In this regard, previously the use of active carbon-based electrodes was demonstrated to be an exciting approach to achieve low voltage channel modulation in EGOFETs.[11] However, carbon-based electrodes have been mainly exploited in transistors with inorganic semiconductors and non-aqueous electrolytes[12,13] or implemented in the so-called organic electrochemical transistors (OECTs),[14,15] which exploit a conducting polymer as the active channel material. Additionally, the chemical functionalization of the gate electrode of EGOFETs for bio-sensing approaches has been limited to the use of self-assembled bio-active molecules grafted on conventional metal gate electrode surfaces.[7]

*[a] Institut de Ciència de Materials de Barcelona (ICMAB-CSIC), Campus de la Universitat Autònoma de Barcelona, 08193 Bellaterra, Spain. E-mail: mmas@icmab.es*

*[b] GENOCOV Research Group, Department of Chemistry, Faculty of Science, Edifici C-Nord, Universitat Autònoma de Barcelona, Carrer dels Til·lers, 08193 Bellaterra (Cerdanyola del Vallès), Barcelona, Spain*

*[c] Networking Research Center on Bioengineering, Biomaterials and Nanomedicine (CIBER-BBN), Campus de la Universitat Autònoma de Barcelona, 08193 Bellaterra, Spain*

† Electronic supplementary information (ESI) available: Experimental procedures and further characterization data. See DOI: 10.1039/c9tc04929k

This journal is © The Royal Society of Chemistry 2019

*J. Mater. Chem. C*, 2019, **7**, 14993–14998 | **14993**

The use of different forms of carbon nanostructures (*i.e.*, carbon nanotubes (CNTs), graphene, graphite and related structures) for the development of nanocomposite carbon paste electrodes (NC-CPEs) has played a leading role in analytical bio-sensing electrochemical devices.[16,17] Specifically, CNTs arise as ideal conducting phase since their dispersion within an inert polymeric matrix is a very attractive way to combine the mechanical, chemical, structural, electrical and tunability properties of individual nanotubes with the processing advantages of polymers.[18,19] NC-CPEs benefit from several intrinsic features, including (i) robustness, (ii) renewable exposed surface by polishing, (iii) ability to customize their electrical properties by modifying the filler/polymer composition ratio and (iv) compatibility with a large variety of functionalization approaches;[20] however, their exploitation in electronic devices is nowadays an unexplored field.

Considering the mentioned advantages of NC-CPEs and motivated by the possibility to widen the current limited library of gate electrodes, a novel EGOFET employing a carbon-based nanocomposite gate terminal is proposed, using CNTs as a model conducting filler. The NC-CPE was fabricated following an easy protocol by dispersing CNTs within an insulating epoxy resin.[21] As a first demonstration of sensing applicability, a functionalized CNT-based NC-CPE with gold nanoparticles (Au-NPs) carrying a thiolated β-cyclodextrin (β-CD) has been developed taking into account the well-known supramolecular complex formation between tryptophan (TRP) and β-CD (see Scheme 1).[22,23] Novelly, this approach achieves a renewable sensing gate surface by a simple polishing step owing to the fact that the bio-recognition unit is included directly in the carbon-paste before the electrode mounting.[24] This approach led to an EGOFET bio-sensor exhibiting an excellent linear response ($10^{-12}$ to $10^{-9}$ M) with a picomolar ($1.0 \pm 0.1$ pM) detection limit.

Hand-made NC-CPEs were fabricated by dispersing different composition ratios of CNTs within the insulating epoxy resin by manual homogenization as explained in the Experimental section in the ESI.†[21] The carbon-paste was then placed into a cylindrical polyvinyl chloride (PVC) tube containing a copper disk to mount the electrode (see Experimental details in ESI†). As shown in Fig. 1A, the percolation curve was constructed by varying the CNT loading from 3% to 20% (w/w). While nanocomposites containing less than 3% of CNTs presented insulating properties with resistivity values $\sim \infty$, those comprising more than 20% of CNTs were not robust enough. Four different zones were distinguished from the percolation curve: (a) high resistance zone composites (HRCs), (b) percolation zone composites (PCs), (c) near-percolation zone composites (NPCs) and (d) low resistivity zone composites (LRCs), where conductivity reaches its maximum. Thus, representative nanocomposite compositions for each zone (3% for HRC, 5% for PC, 10% for NPC and 20% for LRC) were chosen for performing further electrochemical and electronic studies.

The electrochemical performances of the developed NC-CPEs regarding their composition ratios were studied by cyclic voltammetry (CV) and electrochemical impedance spectroscopy (EIS), using $[Fe(CN)_6]^{3-/4-}$ as the redox marker, as summarized in Table 1. The CVs from Fig. 1B reveal information about the accessibility of the redox marker to be oxidized or reduced at the electrode surface by analyzing the peak currents ($I_p$), where the reversibility of the redox couple is defined in terms of the redox peak separation ($\Delta E_p$).[25] Thus, a more reversible electrochemical behavior (lower $\Delta E_p$) also accompanied by higher $I_p$ values was achieved with increasing the CNT loading.[26] This fact



Scheme 1 Schematic procedure of the EGOFET sensing approach. (A) Activated-CNTs containing carboxylic groups were firstly functionalized with Au-NPs as nanotemplates (i) in order to attach the bio-recognition element, a thiolated β-CD (ii). Subsequently, the hybrid nanomaterial was dispersed throughout the polymeric matrix for the NC-CPE fabrication (iii), which after a 10 minute incubation time with different TRP concentrations, was incorporated as a gate electrode into the electronic transistor (iv). (B) Real photographs of the EGOFET setup showing the images of the three individual components and the assembly of these components to build the EGOFET device.
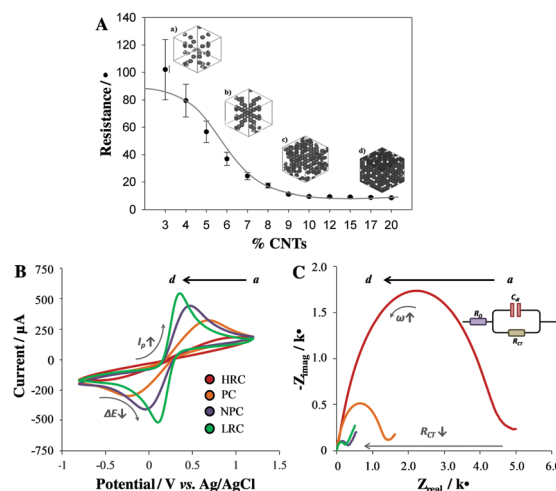


Fig. 1 (A) Percolation curve from the different NC-CPE composition ratios (3% to 20% w/w in CNTs) showing four different regions: (a) HRC (3%), (b) PC (5%), (c) NPC (10%) and (d) LRC (20%). (B) CV and (C) Nyquist plots (inset: equivalent Randles circuit) for the selected NC-CPEs representing the four different percolation regions. Electrochemical experiments were recorded in 0.1 M KCl aqueous solution containing 0.01 M $[Fe(CN)_6]^{3-/4-}$. The scan rate in the CV measurements was 10 mV s$^{-1}$.

**Table 1** Electrochemical parameters for the four different NC-CPE composition ratios obtained by CV ($I_p$, $A$ and $\Delta E_p$) and EIS ($R_\Omega$, $R_{CT}$ and $C_{dl}$)

| CNTs (%) | Percolation zone | $I_p$ ($\mu A$) | $A^a$ ($cm^2$) | $\Delta E_p$ (V) | $R_\Omega$ ($\Omega$) | $R_{CT}$ ($k\Omega$) | $C_{dl}$ ($\mu F$) |
|---|---|---|---|---|---|---|---|
| 3 | HRC | 198 | 0.15 | 0.43 | 866 | 4.5 | 0.44 |
| 5 | PC | 330 | 0.26 | 0.27 | 405 | 1.9 | 1.33 |
| 10 | NPC | 439 | 0.37 | 0.17 | 162 | 0.71 | 4.56 |
| 20 | LRC | 542 | 0.46 | 0.16 | 85 | 0.26 | 9.64 |

$^a$ $A$: electroactive area, which was calculated in terms of peak current ($I_p$, A) and scan rate ($\nu$, V s$^{-1}$), according to the modified Randles–Sevčik equation.[21]

is mainly due to the enhancement of the electroactive area ($A$) with increasing the amount of conducting carbon filler (*i.e.*, CNTs). Thus, the electron transfer rate of the NC-CPEs can be tailored by simply modifying the carbon/polymer composition ratio.

Fig. 1C depicts the Nyquist plots registered for the four selected NC-CPEs, which show the typical semicircle feature characteristic of a Randles cell (see Fig. 1C, inset). The end of the semicircle (low frequency domain) corresponds to the charge transfer resistance ($R_{CT}$), a parameter that is inversely proportional to the electron transfer rate.[27] In agreement with the voltammetric experiments, the $R_{CT}$ value decreases with increasing CNT loading because of the increase of the electroactive sites on the electrode surface. Additional electrochemical parameters related to the EIS performance were also evaluated (Table 1), such as (i) the solution resistance ($R_\Omega$), which is dependent on the ionic concentration and directly related to the dry resistance taken from the percolation curve, and (ii) the

double-layer capacitance ($C_{dl}$), which is directly related to the charging or background current. As expected from the percolation curve, a $R_\Omega$ decrease with increasing CNT loading was observed. This fact can be explained since at lower carbon loads, the ohmic resistance is dominated by the nanocomposite resistance, whereas at higher carbon loads, this parameter is more dominated by the solution resistance.[26] Concerning $C_{dl}$, an increase of the electrode capacitance with increasing the %CNT load was observed since this parameter is determined nearly exclusively by the exposed carbon on the electrode surface.

Subsequently, EGOFETs based on a thin film of the organic semiconductor dibenzo-tetrathiafulvalene (DB-TTF) blended with polystyrene (4% w/w, ratio 1:2) and deposited by bar-assisted meniscus shearing (BAMS) on a flexible Kapton substrate with pre-patterned source–drain electrodes were fabricated as previously reported (see ESI† for further details).[28–30] As the gate terminal, the four types of CNT-based NC-CPEs were employed. Scheme 1 shows the EGOFET configuration. For electronic performance comparison, Pt and glassy carbon (GC) conventional electrodes were utilized.

Transfer and output characteristics were acquired using Milli-Q water as the electrolyte medium (Fig. 2A and Fig. S1, ESI†). All the EGOFETs display a clear p-type modulation and the overall performances of the NC-CPE-based EGOFETs were comparable with the ones achieved with the conventional Pt and GC gates (Fig. 2B and Table 2). It can be noted that the transfer characteristics recorded in the saturation regime ($V_{DS} = -0.4$ V) display a marked $V_{TH}$ shift. Such a $V_{TH}$ trend seems to be directly related with the CNT loading of the gate electrode and, hence, with its intrinsic $C_{dl}$ value derived
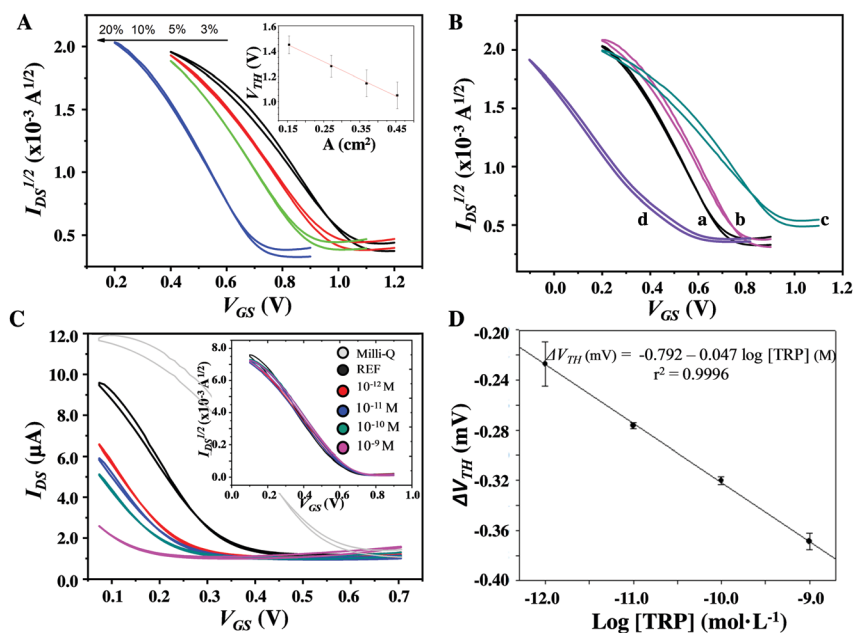


**Fig. 2** (A) *I/V* transfer characteristics of NC-CPEs loaded from 3% to 20% in CNTs (w/w) (inset: correlation $A$ *vs.* $V_{TH}$ of the NC-CPEs). (B) Electrical comparison of EGOFETs employing: (a) raw CNTs and (d) β-CD/Au-NP@CNTs using the optimum NC-CPE composition ratio (20% w/w in carbon filler), and two standard electrodes, (b) GC and (c) Pt. (C) Electrical sensing response of the EGOFET at increasing [TRP] at the bio-recognition gate system. Reference curves present the pre-conditioning step in the electrolyte media (Milli-Q water and the PBS buffer) employed during the experiment (inset: negative EGOFET response at the bare NC-CPE). (D) Calibration curve of $V_{TH}$ *vs.* log [TRP] at the bio-recognition system, which is represented with its corresponding error bars ($n = 9$). Experiments recorded in the saturation regime ($V_{DS} = -0.4$ V).

This journal is © The Royal Society of Chemistry 2019

*J. Mater. Chem. C*, 2019, **7**, 14993–14998 | **14995**

from the electroactive area (A) (Fig. 2A, inset). The regression equation obtained is: $V_{TH}$ (V) = 1.65–1.36 A (cm$^2$) with $r^2$ = 0.996. Leakage current ($I_{GS}$) represents an important feature of EGOFETs and a qualitative indicator of its field-effect operation mode. In the present case, the $I_{GS}$ response remains constant regardless of the type of gate electrode (Fig. S2, ESI†). Moreover, the low $I_{GS}$ current and the almost absent hysteresis suggest that no electrochemical doping is occurring. Importantly, the electrical device properties and, in particular, the operation voltage window, could be successfully modulated with the %CNT loading of the gate NC-CPEs, shifting the $V_{TH}$ up to 0.4 V (see Table 2).

Having determined the excellent electronic behavior of the CNT-based NC-CPEs as novel gate electrodes and taking into account their great potential for applications in bio-sensors, NC-CPEs were exploited for the first time as novel bio-sensing gates in an EGOFET device.[31] In the present case, NC-CPEs containing a 20% load of the conducting filler were selected as the optimum ones due to their lower operational voltage (see Fig. 2A) as well as higher A and $C_{dl}$ values (see Table 1), ensuring an excellent analytical response in the EGOFET device. Accordingly, a renewable bio-recognition sensing gate was developed for L-tryptophan (TRP) determination as a proof of concept, which is a relevant amino acid for humans since it is a neurotransmitter and hormone precursor.[32] For this aim, Au-NPs were incorporated on the CNT walls and afterwards functionalized with a thiolated β-CD (see Experimental section from ESI† and Fig. S3 for the microscopic and X-ray spectroscopy characterizations), which is known to form a host–guest supramolecular complex with TRP.[33] Au-NPs were used as nanotemplates in order to ensure an appropriate orientation of the β-CD empty cavity. Afterwards, NC-CPEs were fabricated by dispersing 20% (w/w) of the functionalized CNT-filler (β-CD/Au-NP@CNTs) throughout the insulating epoxy resin and then applied as a bio-sensing gate for TRP determination. Importantly, this approach allows the development of bio-sensing gate electrodes that can be easily reset by a simple polishing step since the active bio-recognition unit (β-CD) is incorporated into the precursor conducting paste. This aspect represents a unique property of NC-CPEs in comparison with common metal or GC electrodes.[34]

As evidenced in Fig. 2B (curves a vs. d), adding the bio-recognition unit on the paste electrode shifts the transfer characteristics towards more negative values. Sensing performances were carried out by preparing different [TRP] values from $10^{-12}$ to $10^{-9}$ M in a phosphate buffer saline (PBS) solution at pH 7.4. Then,

the gate electrode was immersed in an Eppendorf® tube filled with 1 mL of each solution for 10 min in order to promote the formation of the supramolecular complex between β-CD and TRP and, subsequently, incorporated in the EGOFET. In order to exclude any possible interference coming from the buffer solution, the first experiment before the sensing tests consisted in immersing the functionalized NC-CPE in only PBS for 10 min. A series of 20 transfer scans every 30 s were performed with this gate in Milli-Q water showing a perfect overlap between the initial and final curves (Fig. S4, ESI†) and, hence, demonstrating the stability of the EGOFET device. Such I–V characteristics were also used as reference for the successive measurements.

As it was expected from the impedimetric experiments (see Fig. S5, ESI†), a progressive shift of the transfer characteristics was observed with increasing the [TRP], as shown in Fig. 2C. This behavior could be ascribed to the influence of the dipole moment of TRP on the device electrical characteristics, since it is in a zwitterionic form (p$Ka_1$ = 2.38, and p$Ka_2$ = 9.39) at the working pH.[35] The dipolar moment of the molecules on the gate electrode is known to modify the effective potential applied to the channel.[30] In the present case, the supramolecular interactions formed between TRP and β-CD lead to an effective gate potential decrease. At a fixed $V_{GS}$, a clear decrease of the current in the transfer characteristics is observed with increasing the analyte concentration, being reduced by one order of magnitude at nM concentrations. It should be highlighted that the control experiment carried out with the bare NC-CPE (20% w/w in raw CNTs) did not present any response towards [TRP] due to the absence of the bio-recognition element (Fig. 2C, inset). The sensing properties of these devices were evaluated by extracting $V_{TH}$ from the transfer characteristics in the linear regime ($V_{DS}$ = −0.1 V). The $V_{TH}$ vs. [TRP] calibration curve was constructed per triplicate using three different electrodes (n = 9) in order to evaluate both repeatability of the sensing system after the polishing step and reproducibility during the fabrication process. The calibration curve from Fig. 2D illustrates excellent sensitivity, reproducibility and regression line ($r^2$ = 0.9996), achieving promising analytical results by means of detection limits at picomolar levels (1.0 ± 0.1 pM) as well as a wide range of linear response from $10^{-12}$ to $10^{-9}$ M. Interestingly, while common carbon-based electrochemical sensing devices determine TRP in the nM range, the present approach based on a carbon-based EGOFET platform is capable of achieving the detection of pM concentrations, demonstrating the high sensitivity of the transistor.[36–38] It is also important to point out the renewability of the bio-recognition system by a simple polishing step without losing sensibility. As it is depicted in Fig. S6 (ESI†), the initial EGOFET performance was recovered after the sensing analytical experiments, verifying that the NC-CPE gate electrode can be used again for sensing. All these results elucidate the wide perspectives that NC-CPEs might offer in the field of renewable gates for EGOFET bio-sensing.

## Conclusions

Overall, NC-CPEs have been exploited for the first time in EGOFET technology as novel gate electrodes showing that they

**Table 2** Electrical characteristics of the different gate electrodes employed in this study

| Electrode type | Mobility, $\mu$ (cm$^2$ V$^{-1}$ s$^{-1}$) | $V_{TH}$ (V) |
|---|---|---|
| GC | $2.8 \times 10^{-2}$ ($\pm 0.4 \times 10^{-2}$) | 1.06 ($\pm 0.11$) |
| Pt | $2.9 \times 10^{-2}$ ($\pm 2.7 \times 10^{-2}$) | 1.07 ($\pm 0.34$) |
| NC-CPE (3%) | $0.6 \times 10^{-2}$ ($\pm 0.4 \times 10^{-2}$) | 1.36 ($\pm 0.14$) |
| NC-CPE (5%) | $0.7 \times 10^{-2}$ ($\pm 0.4 \times 10^{-2}$) | 1.24 ($\pm 0.12$) |
| NC-CPE (10%) | $0.8 \times 10^{-2}$ ($\pm 0.4 \times 10^{-2}$) | 1.04 ($\pm 0.15$) |
| NC-CPE (20%) | $1.0 \times 10^{-2}$ ($\pm 0.7 \times 10^{-2}$) | 0.95 ($\pm 0.14$) |
| β-CD/Au-NP@CNTs (20%) | $3.0 \times 10^{-2}$ ($\pm 0.2 \times 10^{-2}$) | 0.50 ($\pm 0.33$) |

Note: % is calculated by means of CNTs (w/w).

can be a good alternative to conventional electrodes. Using CNTs as a model carbon filler, it has been demonstrated that the electrical properties of a transistor can be tailored by changing the filler/polymer composition ratio. It was found that the NC-CPE electroactive area is directly related to the device threshold voltage, and thus, allows for the tuning of the device operation voltage window.

As a proof of concept, a reusable gate has been developed by integrating β-CD within the NC-CPE for TRP determination *via* supramolecular complex formation. Following this route, an EGOFET bio-sensor with an excellent analytical response, exhibiting high sensitivity, wide linear range and a superb limit of detection as low as 1.0 pM, was achieved. Hence, this work can pave the way for widespread applications of NC-CPEs in EGOFETs as new sensitive, reusable, robust and reproducible electronic bio-sensor devices.

## Conflicts of interest

There are no conflicts to declare.

## Acknowledgements

## References

1 T. Cramer, A. Campana, F. Leonardi, S. Casalini, A. Kyndiah, M. Murgia and F. Biscarini, *J. Mater. Chem. B*, 2013, **1**, 3728–3741.

2 L. Kergoat, B. Piro, M. Berggren, G. Horowitz and M.-C. Pham, *Anal. Bioanal. Chem.*, 2012, **402**, 1813–1826.

3 K. Manoli, M. Magliulo, M. Y. Mulla, M. Singh, L. Sabbatini, G. Palazzo and L. Torsi, *Angew. Chem., Int. Ed.*, 2015, **54**, 12562–12576.

4 L. Kergoat, L. Herlogsson, D. Braga, B. Piro, M. C. Pham, X. Crispin, M. Berggren and G. Horowitz, *Adv. Mater.*, 2010, **22**, 2565–2569.

5 G. Foschi, F. Leonardi, A. Scala, F. Biscarini, A. Kovtun, A. Liscio, A. Mazzaglia and S. Casalini, *Nanoscale*, 2015, **7**, 20025–20032.

6 C. Diacci, M. Berto, M. D. Lauro, E. Bianchini, M. Pinti, D. T. Simon, F. Biscarini and C. A. Bortolotti, *Biointerphases*, 2017, **12**, 05F401.

7 D. Wang, V. Noël and B. Piro, *Electronics*, 2016, **5**, 9.

8 E. Macchia, K. Manoli, B. Holzer, C. Di Franco, M. Ghittorelli, F. Torricelli, D. Alberga, G. F. Mangiatordi, G. Palazzo and G. Scamarcio, *Nat. Commun.*, 2018, **9**, 3223.

9 M. Y. Mulla, E. Tuccori, M. Magliulo, G. Lattanzi, G. Palazzo, K. Persaud and L. Torsi, *Nat. Commun.*, 2015, **6**, 6010.

10 S. Casalini, A. C. Dumitru, F. Leonardi, C. A. Bortolotti, E. T. Herruzo, A. Campana, R. F. De Oliveira, T. Cramer, R. Garcia and F. Biscarini, *ACS Nano*, 2015, **9**, 5051–5062.

11 J. Sayago, F. Soavi, Y. Sivalingam, F. Cicoira and C. Santato, *J. Mater. Chem. C*, 2014, **2**, 5690–5694.

12 I. Valitova, P. Kumar, X. Meng, F. Soavi, C. Santato and F. Cicoira, *ACS Appl. Mater. Interfaces*, 2016, **8**, 14855–14862.

13 X. Meng, F. Quenneville, F. d. r. Venne, E. Di Mauro, D. Işık, M. Barbosa, Y. Drolet, M. M. Natile, D. Rochefort and F. Soavi, *J. Phys. Chem. C*, 2015, **119**, 21732–21738.

14 Z. Yi, L. G. Bettini, G. Tomasello, P. Kumar, P. Piseri, I. Valitova, P. Milani, F. Soavi and F. Cicoira, *J. Polym. Sci., Part B: Polym. Phys.*, 2017, **55**, 96–103.

15 H. Tang, P. Kumar, S. Zhang, Z. Yi, G. D. Crescenzo, C. Santato, F. Soavi and F. Cicoira, *ACS Appl. Mater. Interfaces*, 2014, **7**, 969–973.

16 P. M. Ajayan, L. S. Schadler and P. V. Braun, *Nanocomposite science and technology*, John Wiley & Sons, 2006.

17 S. Alwarappan, C. Liu, A. Kumar and C.-Z. Li, *J. Phys. Chem. C*, 2010, **114**, 12920–12924.

18 F. Gardea and D. C. Lagoudas, *Composites, Part B*, 2014, **56**, 611–620.

19 A. Kausar, I. Rafique and B. Muhammad, *Polym.-Plast. Technol. Eng.*, 2016, **55**, 1167–1191.

20 J. Muñoz and M. Baeza, *Electroanalysis*, 2017, **29**, 1660–1669.

21 J. Muñoz, F. Cespedes and M. Baeza, *J. Electrochem. Soc.*, 2015, **162**, B217–B224.

22 G. Xie, W. Tian, L. Wen, K. Xiao, Z. Zhang, Q. Liu, G. Hou, P. Li, Y. Tian and L. Jiang, *Chem. Commun.*, 2015, **51**, 3135–3138.

23 S. Rudolph, E. Riedel and T. Henle, *Eur. Food Res. Technol.*, 2018, **244**, 1511–1519.

24 J. Muñoz, M. Riba-Moliner, L. J. Brennan, Y. K. Gun'ko, F. Céspedes, A. González-Campo and M. Baeza, *Microchim. Acta*, 2016, **183**, 1579–1589.

25 N. V. Rees, *Electrochemistry Fundamentals: Nanomaterials for Fuel Cell Catalysis*, Springer, 2016, pp. 1–29.

26 J. Muñoz, L. J. Brennan, F. Céspedes, Y. K. Gun'ko and M. Baeza, *Compos. Sci. Technol.*, 2016, **125**, 71–79.

27 J. Muñoz, R. Montes and M. Baeza, *TrAC, Trends Anal. Chem.*, 2017, **97**, 201–215.

28 F. Leonardi, S. Casalini, Q. Zhang, S. Galindo, D. Gutiérrez and M. Mas-Torrent, *Adv. Mater.*, 2016, **28**, 10311–10316.

29 I. Temiño, F. G. Del Pozo, M. Ajayakumar, S. Galindo, J. Puigdollers and M. Mas-Torrent, *Adv. Mater. Technol.*, 2016, **1**, 1600090.

30 F. Leonardi, A. Tamayo, S. Casalini and M. Mas-Torrent, *RSC Adv.*, 2018, **8**, 27509–27515.

This journal is © The Royal Society of Chemistry 2019

*J. Mater. Chem. C*, 2019, **7**, 14993–14998 | 14997

31  I. Švancara, K. Vytřas, K. Kalcher, A. Walcarius and J. Wang, *Electroanalysis*, 2009, **21**, 7–28.

32  J. Muñoz, A. González-Campo, M. Riba-Moliner, M. Baeza and M. Mas-Torrent, *Biosens. Bioelectron.*, 2018, **105**, 95–102.

33  J. Han, Q. Wang, J. Zhai, L. Han and S. Dong, *Analyst*, 2015, **140**, 5295–5300.

34  G. Barrett, *Chemistry and biochemistry of the amino acids*, Springer Science & Business Media, 2012.

35  R. Antoine, I. Compagnon, D. Rayane, M. Broyer, P. Dugourd, G. Breaux, F. Hagemeister, D. Pippen, R. Hudgins and M. Jarrold, *Eur. Phys. J. D*, 2002, **20**, 583–587.

36  P. Lei, Y. Zhou, G. Zhang, Y. Zhang, C. Zhang, S. Hong, Y. Yang, C. Dong and S. Shuang, *Talanta*, 2019, **195**, 306–312.

37  W. Liang, Y. Rong, L. Fan, W. Dong, Q. Dong, C. Yang, Z. Zhong, C. Dong, S. Shuang and W.-Y. Wong, *J. Mater. Chem. C*, 2018, **6**, 12822–12829.

38  A. V. Porifreva, V. V. Gorbatchuk, V. G. Evtugyn, I. I. Stoikov and G. A. Evtugyn, *Electroanalysis*, 2018, **30**, 641–649.

**14998** | *J. Mater. Chem. C,* 2019, **7**, 14993–14998

This journal is © The Royal Society of Chemistry 2019